



# ATLAS Inner Detector

## Concept of Radiation Monitor

ATLAS Project Document |No.:

Institute Document |No.:

Created: 06/09/04

Page: 1 of 163

Modified: 4/5/2005 1:01 PM

Rev. |No.: A

### Conceptual Design

## Conceptual Design and Functional Specification of ATLAS Radiation Monitor

*This document outlines the conceptual design considerations and expected functionality of the Radiation Monitor (RM). The RM builds together with Beam Conditioning Monitor (BCM) the ATLAS Radiation Monitoring System.*

Prepared by:

Gregor Kramberger, J. Stefan Institute, Slovenia  
Vladimir Cindro, J. Stefan Institute  
Igor Mandic, J. Stefan Institute  
Marko Mikuz, J. Stefan Institute  
Marko Zavrtanik, J. Stefan Institute

Checked by:

Approved by:

**Comment:** PAGE: 1  
Enter Name, Institute, E-mail

Distribution List

**History of Changes**

| <i>Rev. No.</i> | <i>Date</i>          | <i>Pages</i> | <i>Description of changes</i> |
|-----------------|----------------------|--------------|-------------------------------|
| A               | 06/09/04<br>02/03/05 |              | V 1.0<br>V 1.1                |

## 0 Introduction

This document outlines the conceptual design considerations and expected functionality of the Radiation Monitor (RM) which is the part of the ATLAS Radiation Monitoring System (ARMS). Its goals are

- Measurement of the total ionising dose (**TID**) at various locations in the detector
- Measurement of non-ionising energy loss (NIEL) at various locations in the detector.
- Measurement of the degradation of DMILL bipolar transistors performance in the Inner Detector.

The measurements of TID and NIEL are vital for understanding the changes in performance during the operation of the ATLAS detector, verifying simulations and thus giving a chance to plan a better operation scenario.

It is foreseen that radiation doses will be measured with sensors which can be read out online in the whole ATLAS. The basic unit will be a RM sensor board (RMSB) which will host radiation detectors connected to the readout cables.

In the Inner Detector RMSB will be placed at 12 locations (see section 4) and will provide on-line information of ionization dose in SiO<sub>2</sub>, NIEL in silicon and damage to the DMILL transistors. Because of large range of doses, very limited access, and relatively low number of locations due to limited space, RMSB in the Inner Detector will host a number of radiation detectors which will cover the large range of doses and provide a high level of redundancy.

Outside Inner detector TID and NIEL damage will be measured at large number of locations (~200) with simpler RMSBs containing only two sensors, one for each type of radiation damage (TID and NIEL).

## 1 Detectors

To provide above functionality detectors sensitive to various radiation types will be used.

### 1.1 DOSE measurement

#### 1.1.1 RADFETS

The on-line measurement of the **Total Ionising Dose** (TID) is nowadays most commonly [1,2] performed with **Radiation Field Effect Transistors** (RADFET).

The measurement technique exploits the change of the threshold voltage (voltage needed at the gate of the transistor to achieve conduction) due to irradiation in p-MOS transistors. The radiation induced electrons and holes have different mobilities in the oxide and while electrons are collected by the gate electrode the holes are trapped in the oxide or at the oxide-silicon surface. Consequent change in electric field must be compensated by a larger negative gate voltage  $V_G$  needed to open the channel. Therefore, the increase of the gate voltage at fixed drain current is the measure of the received dose. The crucial parameter of the RADFET is the oxide thickness as it determines the sensitivity and dynamic range. RADFETs with thin oxide (~100 nm) are suitable for measurements of larger doses, however with smaller sensitivity, while thicker oxide allows higher sensitivity at smaller range as the increase of  $V_G$  becomes the limiting parameter.

A RADFET has 3 connections (gate, source, drain). In the most usual configuration gate and drain are common, so a RADFET can be read-out using 2 contacts. The read-out is done by applying constant current between the two contacts and measuring the voltage drop. The typical currents are in the range of few hundred  $\mu\text{A}$ . The actual value of current is chosen in such a way that the voltage drop is least dependent on temperature. Typical voltage drops for the Mrad-RADFETs are below 30 V with typical break-down voltages of around 70 V. The voltage drop changes with time after setting the bias, therefore it is important to use the same read-out cycle (apply I, measure V few seconds later) as during calibration. Response curves of RADFETs with different sensitivity can be seen in Fig 1.

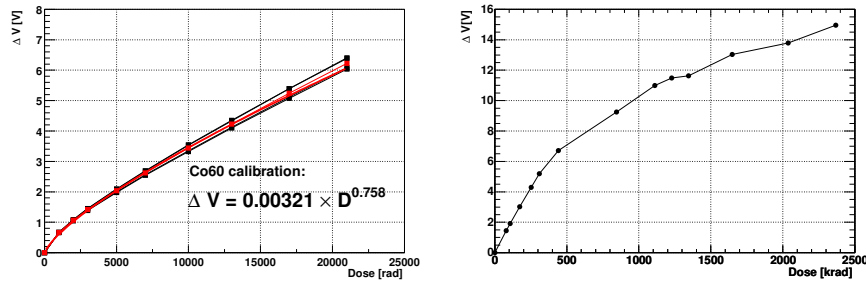


Fig.1 Left: Example of voltage shift vs. dose curve for high sensitivity RADFET obtained with calibrated  $^{60}\text{Co}$  source. Right: Voltage vs. dose of a low sensitivity RADFET exposed to background ionizing radiation in reactor.

RADFETs are available in various packages or as bare chips. Decision on the type, packaging and the producer of the RADFET sensors will be taken after intensive tests being carried out at CERN in the framework of common LHC activity.

## 1.2 Bulk damage (NIEL) measurement

### 1.2.1 Leakage current measurements of pad-detectors (diodes)

The bulk damage in silicon has been studied in great detail by ROSE (RD48) collaboration [3]. The leakage current increase ( $\Delta I$ ) after irradiation has been found to be directly proportional to Non-ionising Energy Loss (NIEL) and independent on the material type (same for diffusion oxygenated and standard float zone sensors, Chochralsky and epitaxial Si sensors). The 1 MeV neutron equivalent fluence ( $\Phi_{eq}$ ) is determined from  $\frac{\Delta I}{\alpha(t,T) \cdot V} = \phi_{eq}$ , where  $\alpha(t,T)$  is the leakage current damage constant and  $V$  the sensitive volume of the detector. An important fact is also that the annealing of the leakage current (change of  $\alpha$  with time after irradiation) at different temperatures is well known.

A silicon pad detector-diode with a guard ring structure ( $0.5 \times 0.5 \text{ cm}^2$ ) will be used to measure the leakage current increase. In order to have detectors fully depleted already at voltages below 30 V a very thin detectors will be used: 25  $\mu\text{m}$  thick detectors processed on epitaxial silicon of 50  $\Omega\text{cm}$  are foreseen [4]. These detectors invert at  $\Phi > 10^{15} \text{ cm}^{-2}$ , which ensures full depletion during the lifetime of the experiment. The leakage current anneals with time, a strongly temperature dependent process. Most of the experimental studies have been so far done at  $> 20^\circ\text{C}$ . Therefore we propose to mount a controlled resistive heater on the RMSB which will maintain constant temperature of the sensor board.

At larger radii where the estimated fluence received by the detectors is of order  $10^{11} \text{ cm}^{-2}/\text{year}$  standard 300 mm thick sensors with high initial resistivity (15 k $\Omega\text{ cm}$ ,  $V_{FD} \sim 15 \text{ V}$ ) could be used.

To prove the principle we irradiated four 25  $\mu\text{m}$  Epi-Si samples with reactor neutrons to three different equivalent fluences:  $2 \times 10^{13} \text{ cm}^{-2}$ ,  $10^{14} \text{ cm}^{-2}$  and  $2 \times 10^{14} \text{ cm}^{-2}$ . After irradiation the diodes were stored for about a month at  $-17^\circ\text{C}$  (**note** that annealing at higher temperatures was not performed yet). An example of a capacitance-voltage characteristic (C-V) and current-voltage characteristic is shown in Fig. 2. The measurements were performed in a probe-station.

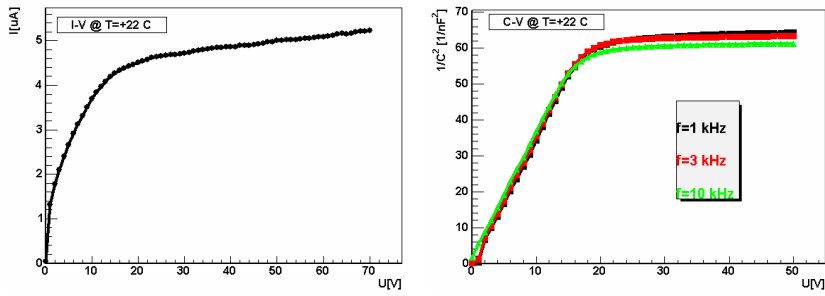


Fig. 2: I-V (left) and C-V (right) characteristics of a 25  $\mu\text{m}$  Epi-Si diode irradiated to equivalent fluence of  $10^{14} \text{ n/cm}^2$

The dependence of full depletion voltage and leakage current (normalized to 20°C) on fluence is shown in Fig. 3. It is clear that 28 V will be sufficient to fully deplete the detector over the entire period of operation. As the leakage current decreases by roughly factor of 2 when temperature is reduced by 7°C it is clear that measurements at higher temperatures yield larger sensitivity. This is particularly important for running at low luminosity where only approximately 1.5% of the final fluence will be received per year. Annealing studies on these samples are under way.

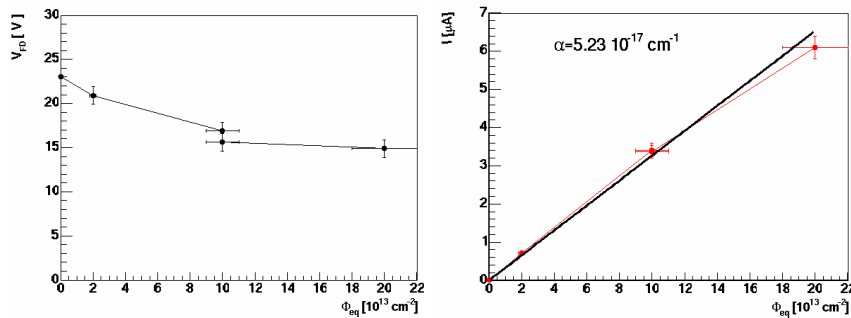


Fig. 3: Full depletion voltage (left) and leakage current normalized to 20°C (right) as a function of equivalent fluence.

### 1.2.2 Measurement of forward bias in PIN diodes

The voltage drop on the intrinsic base of PIN diodes, when operated in forward bias, depends on the minority carrier lifetime. As a consequence of bulk damage, minority carrier lifetime is decreased which increases voltage drop on the intrinsic base. Measurement of forward bias at given forward current can be used to measure bulk damage in silicon [5]. Sensitivity to radiation increases with the width of intrinsic base.

Commercial pin diodes (OSRAM – BPW34F) operated under forward bias seem to be a very promising candidate for measurements of the NIEL equivalent bulk damage. Forward bias at 1 mA of forward current is used as the measure of damage. First tests [6,7] show that these diodes can be used to measure fluences larger than  $5 \times 10^{12} \text{ n/cm}^2$  and that 30 V will be enough to be able to measure equivalent fluences up to  $3 \times 10^{14} \text{ n/cm}^2$ .

More sensitive silicon PIN diodes provided by CMRP, Wollongong Australia [8] will be used for measurements of bulk damage for fluences in the range between few times  $10^{10} \text{ n/cm}^2$  to few times  $10^{12} \text{ n/cm}^2$ .

Several BPW-34F diodes and one high sensitivity diode were irradiated with neutrons in the TRIGA reactor in Ljubljana. Increase of forward voltage at 1 mA forward current as a function of reactor neutron fluence expressed in 1 MeV neutrons NIEL equivalent in Si is shown in Fig. 4.

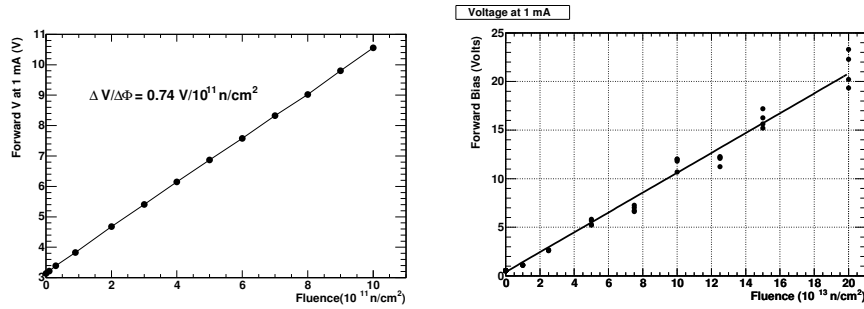


Fig. 4: Forward voltage vs. 1 MeV neutron fluence immediately after irradiation for high sensitivity diode (left) and for BPW-34F diodes (right).

Forward voltage after irradiation anneals with time if diodes are kept at 20°C, which is the planned operating temperature of RMSBs in ATLAS. Annealing studies at different temperatures, have been started and first results are shown in Fig. 5.

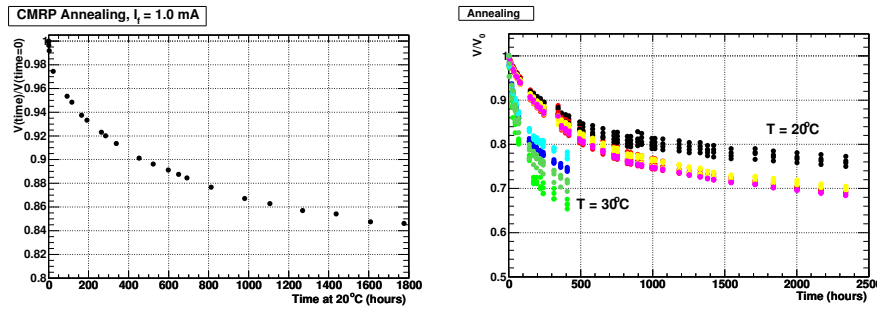


Fig. 5.: Annealing of forward voltage at 1 mA forward current with time after irradiation for high sensitivity diode irradiated to 10<sup>12</sup> n/cm<sup>2</sup> (left) and for several BPW-34F diodes irradiated to different fluences ranging from 10<sup>13</sup> n/cm<sup>2</sup> to 2x10<sup>14</sup> n/cm<sup>2</sup> (right).

### 1.3 DMILL test structures measurements

DMILL bipolar transistors are used in SCT and TRT front-end electronics. Bipolar transistors are sensitive to both, bulk and ionisation damage, which cause degradation of common emitter current gain factor  $\beta = I_c/I_b$  (collector current/base current). The reduction of  $\beta$  is the main cause for degradation of performance (smaller gain, larger noise) of bipolar front-end electronics used in the Inner Detector. It is therefore important to have information about the condition of DMILL transistors, to understand the performance of readout electronics.

In addition, it is a feature of DMILL transistors, that their  $\beta$  is very sensitive also to thermal neutrons [9].

Thermal neutrons contribute only very little to NIEL in pure silicon. But they can cause serious damage to bipolar transistors with boron-doped base. The He and Li ions from reaction  $B + \text{thermal-n} \rightarrow Li + He + \gamma$ , can cause substantial bulk damage within their small range (5  $\mu\text{m}$ ). This reaction is important

because of its large cross section. In [9] it was shown that DMILL bipolar transistors are very sensitive to this kind of damage. It was shown also that the damage caused by fast hadrons and thermal neutrons is additive. From measurement of change of common emitter current gain (i.e. base current increase at given collector current) in DMILL transistors the fluence of thermal neutrons can be measured, if NIEL equivalent fluence is known, because:

$$\frac{\Delta I_b}{I_c} = k_{eq} \cdot \Phi_{eq} + k_{th} \cdot \Phi_{th},$$

where  $k_{eq}$  and  $k_{th}$  are equivalent and thermal neutron damage factors, respectively. Damage factors are measured in calibration irradiations as shown in Fig. 6.

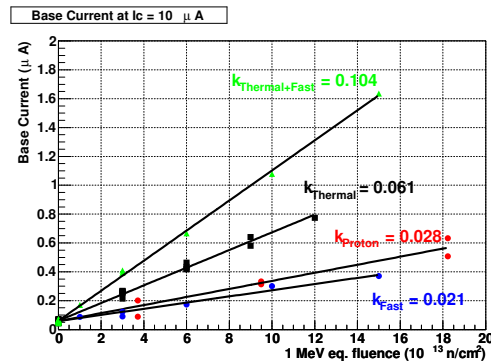


Fig. 6: Base current at 10  $\mu$ A collector current (proportional to  $1/\beta$ ) as a function of fluence. For protons, fast neutrons and for mixture (thermal+fast,  $\Phi_f/\Phi_{th} \sim 0.7$ ) fluence is in 1 MeV equivalent neutrons. For thermal neutrons x-axis means the fluence of thermal neutrons.

It is therefore essential to monitor thermal neutron fluence or to use DMILL test structures (transistors) to get the most reliable estimate on damage inflicted to SCT and TRT front-end electronics. The latter can be used also to estimate fluence of thermal neutrons in the Inner Detector.

DMILL test structures will be mounted on the RMSB to monitor the degradation of  $\beta = I_c/I_b$  (collector current/base current) parameter.

## 2 RMSB Read-out

The general requirement for the read-out of the sensors is that they should be read-out using standard ELMB [10,11] +DAC boards. This saves enormous effort in building a dedicated read-out system and ensures full compatibility, spare parts availability and easy integration into the ATLAS DCS system. On the other hand this reduces to some extent the flexibility of the RMSB. In the following text the more complex RMSB for the Inner Detector will be described. The “rest-of-ATLAS” version will use very similar readout system but with smaller number of components per board.

### 2.1 Design

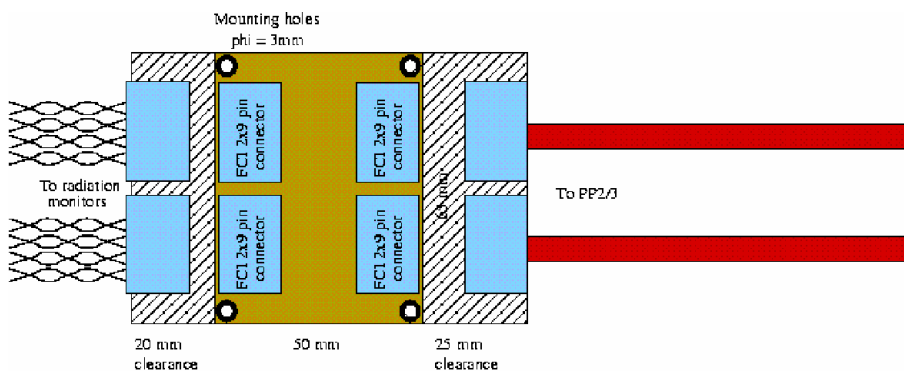
The readout of the RMSB is based on ELMB, which communicates over the CAN bus with ATLAS DCS. Each ELMB hosts 64 12-bit ADC channels (0-4.5 V) with the conversion frequency ranging from 2-100 Hz. Up to four 16 channel 12-bit DAC boards can be connected to and controlled by the ELMB.

The output from ELMB-DAC [12] is current, which can be converted, if needed, to voltage via a resistor. External power supply with max. voltage of 30 V can be connected to DAC boards. The boards can be

operated in two modes: low/0-1mA or high/0-20 mA. When operated in the mode of operation suitable for RADMON purposes (0-1 mA at the output) a maximum voltage drop that can be maintained between the contacts of the DAC channel is 28 V.

### 2.1.1 Connection

The sensor boards will be connected to ELMB by a SCT module TYPE II cable (PP3-PP1, < 12 m) and twisted pair cable from PP1 to RMSB where it will be soldered to the hybrid. FCI connectors will do the connection at PP1 as shown in the Fig. 7.



PPB1-RM  
Ver 0.1  
Conceptual design and dimensions

Fig. 7: Connections of twisted pairs to TYPE-II cable at Patch Panel 1.

TYPE II cable:

- 12 thin wires ( $R=0.22 \Omega/m$ )
- 4 thick wires ( $R=0.033 \Omega/m$ )

### 2.1.2 RMSB Detector Layout

The number of wires constrains the number of sensors hosted by a single RMSB in the Inner Detector. The foreseen layout is shown in Fig. 8 and consists of:

- Epi-Si thin diode (3 wires, 1 DAC, 2 ADC)
- 1 high sensitivity pin diode (1 wire, 1 DAC, 1 ADC)
- 1 BPW-34F pin diode (1 wire, 1 DAC, 1 ADC)
- 2 RADFETs with thin oxide (sensitive up to 20 Mrads) and a RADFET with thicker oxide (sensitive up to few hundred kRads) (3 wires, 3 DAC, 3 ADC)
- DMILL test structure (bipolar transistor) (2 wires, 1 DAC, 2 ADC)
- Temperature sensor (NTC) (1 wire, 1 ADC)
- Heater (2 wires, 1 DAC (+ N DAC if heater is powered by DAC))
- Return (GND) connection (1 wire)
- 2 spare wires, 2 DAC, 2 ADC



The 2 spare wires can be used for additional RADFETs, pin diodes or a DMILL structure. Each RMSB (with maximal number of sensors) will require 10 DAC channels and 12 ADC channels. A careful choice of resistors R1 to R6 is needed to comply with the specification of the ELMB DAC and ADC.

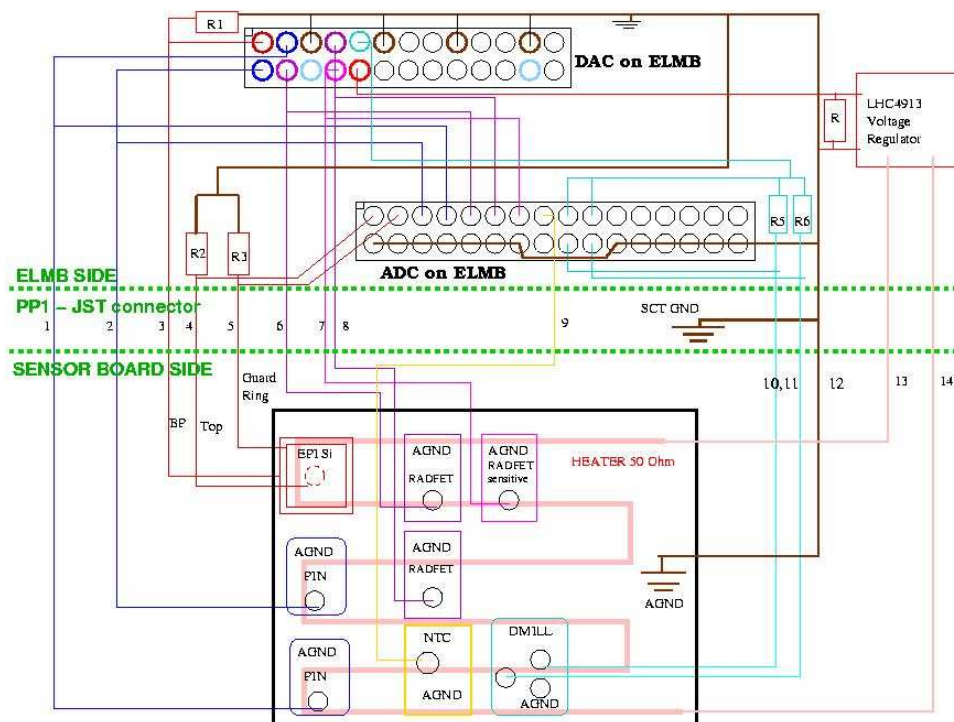


Fig. 8: Readout architecture and layout of the Inner Detector RMSB. In this layout it is foreseen that heater is powered by the LHC4913 voltage regulator.

### 2.1.3 Details about readout of radiation sensors

- EPI-Si diodes: the expected bulk leakage current after 10 years of LHC operation is below  $10 \mu\text{A}$ . It is reasonable to assume that guard ring current will not exceed this value. As the DAC output current is converted to desired voltage by connecting an output resistor R1, it is important to ensure that current flowing through R2 and R3 is much smaller than the one through R1. If  $R1 = 40 \text{ k}\Omega$  the max DAC current will be  $700 \mu\text{A}$  which is  $>35$  times more than expected currents through R2 and R3. Thus a stable voltage is ensured at the diode. To prevent large voltage drop on R2 and R3 it is important to select values as low as possible. On the other hand the voltage drop must be sufficient to yield good ADC resolution. A value around  $100 \text{ k}\Omega$  seems to be a reasonable choice. R2 and R3 could also be replaced during detector operation of detector to restore the optimal solution.
- PIN diodes: a current pulse  $\leq 1 \text{ mA}$  will be injected and voltage drop measured between the contacts of the DAC. The range of the ADC is  $\sim 5 \text{ V}$  max. therefore a differential attenuator will be used (see Fig. 10). To reduce the input impedance of the ADC channel (hence the noise)

capacitors will be used along with the resistors. A choice of very high resistor (high resistance of the voltmeter) is governed by the fact that ground loop currents must be small in order not to disturb the measurement.

- RADFETs: readout is similar to the readout of the PIN diodes with somewhat smaller current injected. Same differential attenuators as for the PIN diodes will be used.
- DMILL structures: Degradation of  $\beta=I_c/I_b$  will be measured. The base current must be measured at given collector current. As the  $I_b < I_c$  a single DAC can be used in the circuit realized in Fig. 2 (cyan). The values of resistors R5 and R6 should be chosen to meet the ADC range.
- NTC temperature sensor will be used.
- Heater: to ensure constant and controlled temperature of the RMSB resistive heaters will be processed directly on the backside of the hybrid. Power to the heater will be provided by radiation hard voltage regulator LHC4913. The regulator will be connected to 12 V input voltage and the output voltage ranging from 0 to 10 V will be controlled by a DAC. The heater must be able to maintain a maximum temperature difference of  $\sim 40^\circ\text{C}$ . Measurements show that such temperature difference can be maintained with 1.2 W heating power. To allow for some overhead, heater resistance will be  $\sim 50 \Omega$  so that a power of 2 W could be achieved with 10 V supply voltage. Results of measurement of temperature difference vs. heater power can be seen in Fig. 9.

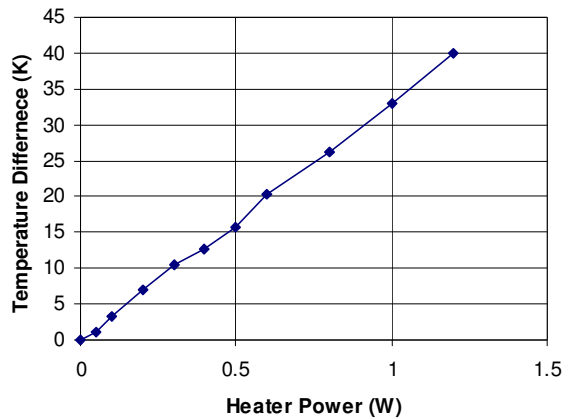


Fig 9: Hybrid temperature vs. power provided to the heater.

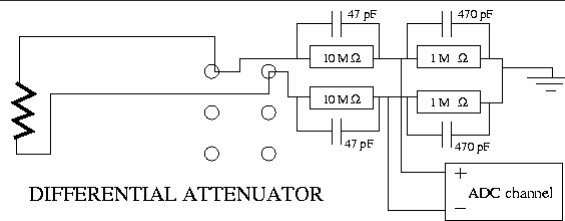


Figure10: Differential attenuator 1:11 that will be used for RADMON purposes.

All resistors (R1 to R6) as well as the differential attenuator and other resistor networks (NTC readout) will be built as dedicated “signal adapters” which will fit the DIL sockets on the ELMB motherboards.

## 2.2 RSMB hybrid

An aluminium oxide ( $\text{Al}_2\text{O}_3$ ) hybrid will ensure mechanical support and temperature stability for the sensors. Its good heat conductivity and high electrical resistance make it an appropriate candidate. Conductive lines of few hundred microns on both sides of  $\sim 600 \mu\text{m}$  thick substrate can be made as well as gold plating to ensure a wire-bondable contacts. Heater lines will be made on one side of the hybrid while sensors will be mounted on the other. Layout of the prototype can be seen in Fig. 11. The contacts on the ceramics will be soldered to a PCB frame with thin wires and the twisted-pairs will be soldered to the PCB frame. The PCB frame with hybrid will be placed in a housing made from PEEK plastic which will mechanically protect the sensors. PEEK was chosen because it is qualified for usage in radiation environment.

The size limit of the RMSB housing is  $40 \times 40 \times 8 \text{ mm}^3$ . Bottom part of housings of RMSB which will be glued to the Pixel Support Tube will be milled to the same radius as the tube. Drawing of the housing is shown in Fig 12.

The hybrid and housing will be made by IJS and the PCB by ElgoLine. The photo of the populated prototype in the housing can be seen in Fig. 13.

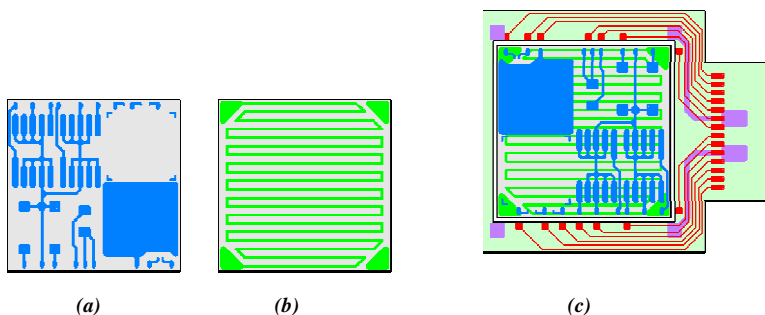


Figure 11: The mask of the prototype hybrid. In Figure (a) the top side of ceramic hybrid is shown with sensor pads and in (b) the bottom side with heater lines. Fig (c) shows the ceramic hybrid in a PCB frame.

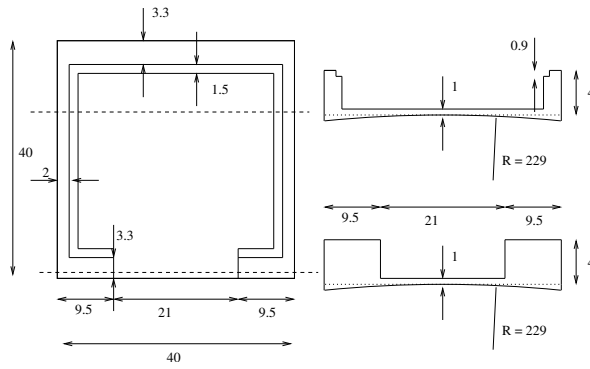


Figure 12: Drawing of the RMSB housing. Bottom parts of housings which will be glued to Pixel Support Tube will be milled to the tube raduys (229 mm). Others will be made flat.

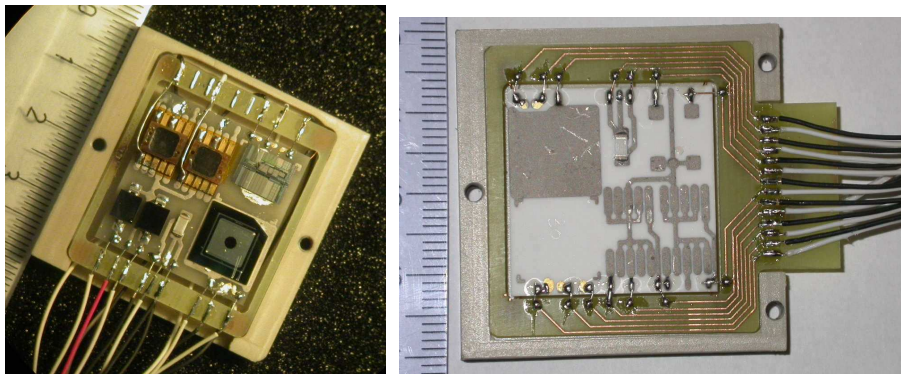


Fig 13: Left: populated hybrid connected to a PCB frame in the bottom part of PEEK housing. Right: Al<sub>203</sub> hybrid in new PCB frame and PEEK box.

### 3 RM layout and location of system components

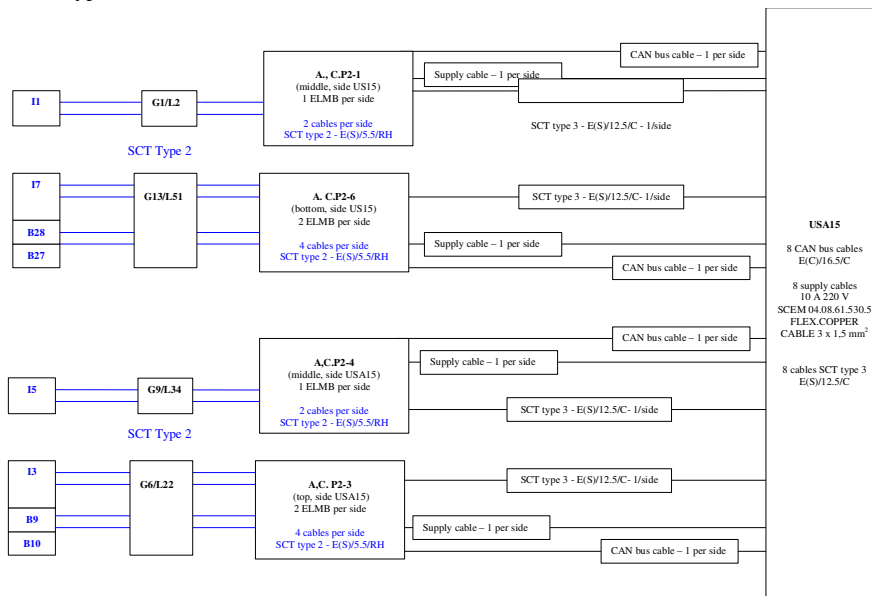
The RMSB in the present configuration will host only sensors. All other components (resistors, capacitors)

will reside at the ELMB side. In the table below the locations of components of the Inner Detector radiation monitor are specified. Number of sensor boards and their location outside of ATLAS detector remains to be defined.

| Component                              | Location and constraints   |                                  |   |                                  |   |                 |       |         |      |      |     |       |         |      |      |      |       |       |      |     |    |
|--|--|----------------------------------|---|----------------------------------|---|-----------------|-------|---------|------|------|-----|-------|---------|------|------|------|-------|-------|------|-----|----|
| RMSB                                   | <p>There will be 12 RMSB in the Inner Detector.</p> <p>In side A boards will be at <math>\Phi = 0^\circ</math> and <math>180^\circ</math> and in side C at <math>\Phi = 90^\circ</math> and <math>270^\circ</math>.</p> <p>There will be 3 boards at each <math>\Phi</math> with (r,z) coordinates given below:</p> <table border="1"> <thead> <tr> <th>r[cm]</th> <th>z [cm]</th> <th><math>\Phi_{eq}[10^{14}/\text{cm}^2]</math></th> <th><math>\Phi[10^{14}/\text{cm}^2]</math><br/>(<math>&gt;20</math> MeV h)</th> <th>TID[<math>10^4</math> Gy]</th> </tr> </thead> <tbody> <tr> <td>40-50</td> <td>340-350</td> <td>2.35</td> <td>1.25</td> <td>6.7</td> </tr> <tr> <td>80-90</td> <td>340-350</td> <td>1.06</td> <td>0.41</td> <td>1.91</td> </tr> <tr> <td>20-30</td> <td>80-90</td> <td>2.33</td> <td>2.2</td> <td>14</td> </tr> </tbody> </table> | r[cm]                            | z [cm]  | $\Phi_{eq}[10^{14}/\text{cm}^2]$ | $\Phi[10^{14}/\text{cm}^2]$<br>( $>20$ MeV h) | TID[ $10^4$ Gy] | 40-50 | 340-350 | 2.35 | 1.25 | 6.7 | 80-90 | 340-350 | 1.06 | 0.41 | 1.91 | 20-30 | 80-90 | 2.33 | 2.2 | 14 |
| r[cm]                                  | z [cm]   | $\Phi_{eq}[10^{14}/\text{cm}^2]$ | $\Phi[10^{14}/\text{cm}^2]$<br>( $>20$ MeV h) | TID[ $10^4$ Gy]                  |   |                 |       |         |      |      |     |       |         |      |      |      |       |       |      |     |    |
| 40-50                                  | 340-350  | 2.35                             | 1.25  | 6.7                              |   |                 |       |         |      |      |     |       |         |      |      |      |       |       |      |     |    |
| 80-90                                  | 340-350  | 1.06                             | 0.41  | 1.91                             |   |                 |       |         |      |      |     |       |         |      |      |      |       |       |      |     |    |
| 20-30                                  | 80-90  | 2.33                             | 2.2   | 14                               |   |                 |       |         |      |      |     |       |         |      |      |      |       |       |      |     |    |
| ELMB                                   | <p>There will be 3 RMSB per ELMB with 3 DAC boards.</p> <p>ELMB will be located next to pixel PP2 behind first muon-layer. In total maximum 4 ELMB+ELMB motherboards.</p>  |                                  |   |                                  |   |                 |       |         |      |      |     |       |         |      |      |      |       |       |      |     |    |
| ELMB power supply and DAC power supply | <p>UX15 (4 ELMB powered by level 0 ID ELMB power supply and 4 ELMB powered by level 8 ID ELMB power supply). Cable for DAC power supply will be routed together with CAN bus cable.</p>  |                                  |   |                                  |   |                 |       |         |      |      |     |       |         |      |      |      |       |       |      |     |    |

#### 4 Cabling

Cabling scheme for the system with 24 RMSBs is shown below. Needs to be revised for the 12 RMSB. Cable types will remain the same.



RM Cabling Schematic – draft 0.1, 17/11/2004 M.Mikuž, adapted from drawing by M. Stodulski  
 Routing gaps, PP2 positions subject to change  
 If rerouting of 11, 15 to 13, 17 on ID plate possible, reduce all services from PP2 – USA15 by 1/2, ELMB 3 to 2/side

## 5 Cost estimates

Cost estimate:

Worst case per inner detector monitoring board:

1. epi-diode 1x 25 CHF = 25 CHF
2. BPW34F PIN diode 2x 5 CHF = 10 CHF
3. CMRP PIN diode 2x 120 CHF = 240 CHF
4. thin oxide radfet 2x 50 CHF = 100 CHF
5. thick oxide radfet 1x 60 CHF = 60 CHF
6. DMILL transistor 2x 25 CHF = 50 CHF
7. NTC 1x 10 CHF = 10 CHF
8. Ceramic hybrid 1x 200 CHF = 200 CHF
9. PEEK housing 1x 100 CHF = 100 CHF
- 10.ELMB 0.5x 200 CHF = 100 CHF
- 11.DAC 16x 22 CHF = 352 CHF
- 12.RMSB-PP2 connect 1x 170 CHF = 170 CHF

TOTAL 1390 CHF

Allowing for some overhead gives price per channel 1.5 kCHF.

For monitors outside the ID only two sensors are foreseen:

- thick oxide radfet : 1x 60 CHF = 60
- CMRP PIN diode : 1x120 CHF = 120
- Temperature sensor : 1x 10 CHF = 10
- ELMB :0.25x200 CHF = 50
- DAC : 4x22 CHF = 88
- RMSB-ELMB connect :0.25x170 CHF = 43
- Housing :0.25x100 CHF = 25
- board :0.25x200 CHF = 50

TOTAL: 446 CHF

## 6 First tests

A simple test stand was constructed (see Fig. 14) to test the read-out of different sensor types. Since the DAC modules are not yet available Keithley-220 current source and a switching matrix was used to provide currents up to 1 mA to the sensors on the hybrid. The CAN-BUS cable was connected to a PC running CANopen-OPC server. A root based OPC client was used instead of the PVSSII for the data taking. All sensors could be read out successfully with this system.

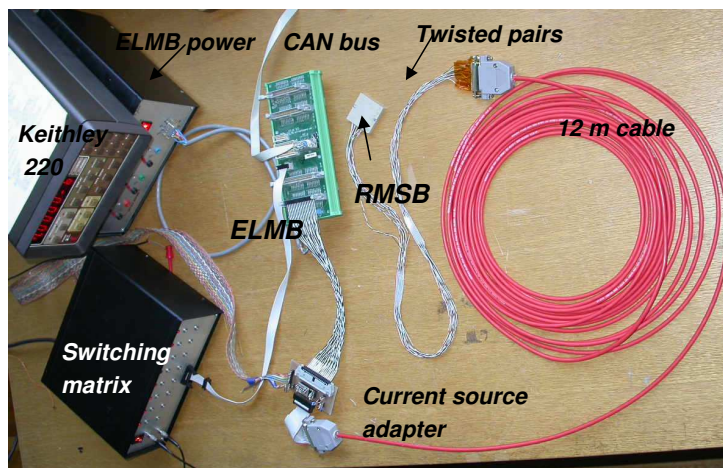


Figure 14: A "prototype" setup.

## References

- [1] D. Dannheim et. al, "A Radiation Monitor for the ZEUS Detector at HERA", presented at IEEE-TNS conference Portland 2003.
- [2] D. Žontar, "Radiation monitoring at Belle", NIM A 501 (2003) 164.
- [3] G. Kramberger et. al, "Superior radiation tolerance of thin epitaxial silicon detectors", NIM A515 (2003) 665.
- [4] G. Lindström et al., "Radiation hard silicon detectors - developments by the RD48 (ROSE) collaboration", NIM A466 (2001) 308.
- [5] J. M. Swartz and M. O. Thurston, "Analysis of the Effect of Fast-Neutron Bombardment on the Current-Voltage Characteristic of a Conductivity-Modulated p-i-n Diode", J. Appl. Phys., Vol. 37, (1966) pp 744.
- [6] M. Tavel, M.E. Leon-Florian, "Dose and neutron-fluence measurements in mixed gamma-neutron fields by means of semiconductor dosimeters" (IEEE Catalogue RADECS '93, St. Malo, France, 1993, pp. 27-32.
- [7] F. Ravotti et al., "Conception of an Integrated Sensor for the Radiation Monitoring of the CMS Experiment at the Large Hadron Collider", CERN-PH-EP/2004-04
- [8] <http://mrp.uow.edu.au/index.shtml>
- [9] I. Mandić et al., "Bulk Damage in DMILL npn Bipolar Transistors Caused by Thermal Neutrons Versus Protons and Fast Neutrons", IEEE TNS, Vol. 51, August 2004, pp 1752.
- [10] ATI-DC-ELMB-001
- [11] ATI-DC-ELMB-002
- [12] [www.nikhef.nl/pub/departments/ct/po/html/ELMB/DAC10.pdf](http://www.nikhef.nl/pub/departments/ct/po/html/ELMB/DAC10.pdf)

## 7 APPENDIX A

DMILL readout circuitry as used for transistor measurements on the probe station is shown in Fig. 15. Very similar circuitry is placed on the “current source adapter” shown in Fig. 14, except that ELMB-ADC is used instead of Voltcraft DVM and KEITHLEY 220 instead of KEITHLEY 220.

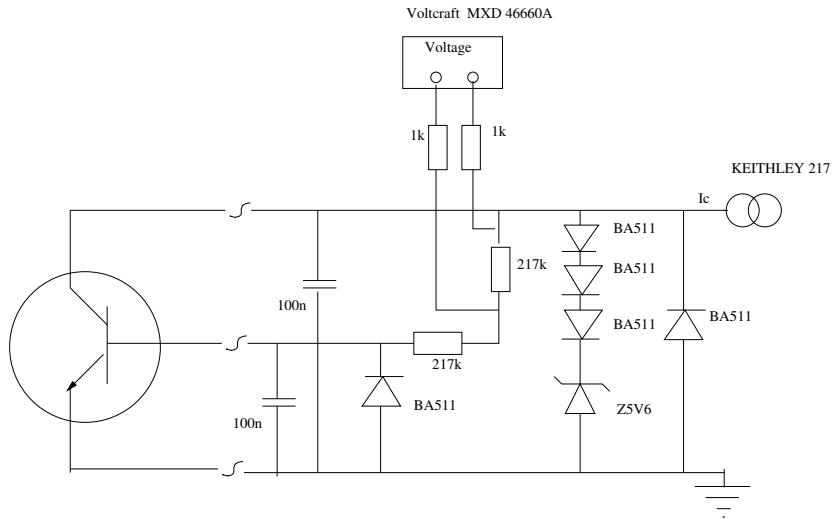


Fig. 15: DMILL transistor readout circuitry.